MOTION CAPTURE OF AN ANIMATED SURFACE VIA SENSORS' RIBBONS

Surface Reconstruction via Tangential Measurements

Nathalie Sprynski
CEA-LETI, MINATEC Campus, Grenoble, France

Bernard Lacolle, Luc Biard
Laboratoire Jean Kuntzmann, Université Joseph Fourier, Grenoble, France

Keywords: Motion capture, Micro-sensors, Surface reconstruction, Curve reconstruction, Hermite interpolation.

Abstract: This paper deals with the motion capture of physical surfaces via a curve acquisition device. This device is a ribbon of sensors, named Ribbon Device, providing tangential measurements, allowing to reconstruct its 3D shape via an existing geometric method. We focus here on the problem of reconstructing animated surfaces, from a finite number of curves running on these surfaces, acquired with the Ribbon Device. This network of spatial curves is organized according a comb structure allowing to adjust these curves with respect to a reference curve, and then to develop a global C1 reconstruction method based on the mesh of ribbon curves together with interpolating transversal curves. Precisely, at each time position the surface is computed from the previous step by an updating process.

1 INTRODUCTION

We are concerned with the reverse engineering problem of re–constructing animated physical surfaces from tangential data. These tangential data are provided by embedded sensors (micro–accelerometers and micro–magnetometers) along a curve represented by a ribbon. This problem is not a *dual* interpolation or approximation problem (Hoschek, 1983) as the tangential data are not localized in space. Appropriate methods for the reconstruction of planar and spatial curves from such tangential information have been developed in (Sprynski et al., 2007) and have been validated by a real-time demonstrator: a ribbon–like device, denoted *Ribbon Device* – see Figure 1 – equipped with 32 micro–sensors. See also (Hoshi and Shinoda, 2008) for a prototype of sensing device, analogous to a rectangular grid of linear instrumented segments, providing thus elementary geometry.

The deep novelty of such capture/reconstruction approaches is to deal with purely orientation data. Furthermore, notice that all previous related works only consider static surfaces. We are thus concerned in this paper with the motion capture of a surface in deformation from a network of spatial curves running on the surface, obtained with the *Ribbon Device*. Precisely, by placing the *Ribbon Device* on a physical surface at regular intervals, the surface is divided into a system of patches, which can be then filled by interpolating Coons processes (Coons, 1964; Coons, 1974; Farin, 2002). See also (Peters, 1990; Sarraga, 1987; Shirman and Séquin, 1987) for construction processes of smooth surfaces from given boundary curve data. The shape of the surface is thus essentially modeled by these spatial curves forming a characteristic mesh of the surface.

Applications are countless, ranging from medical applications (e.g. determining shape and curvature of the spinal column), to aerodynamic applications (e.g. acquiring the shape and deformation of a wing).

This document is organized as follows. The sensors, the acquisition tool and the process used for surface capture are detailed in Section 2. Section 3 focuses on the algorithms developed to solve the problem, which first consists in reconstructing the ribbon curves, and then the interpolating surface. Finally, Section 4 deals with the validation and the implementation.

Sprynski N., Lacolle B. and Biard L..
MOTION CAPTURE OF AN ANIMATED SURFACE VIA SENSORS' RIBBONS - Surface Reconstruction via Tangential Measurements.
DOI: 10.5220/0003330604210426
In *Proceedings of the 1st International Conference on Pervasive and Embedded Computing and Communication Systems* (PECCS-2011), pages 421-426
ISBN: 978-989-8425-48-5

2 ACQUISITION STEPS

2.1 The Acquisition Tool

What is targeted here is to introduce new kinds of instrumented materials. We think for example about plastic or textile ribbons or surfaces, which will be equipped with arrays of sensors in order to gain some new properties. The alliance between instrumented materials and mathematical algorithms will allow materials to be able to access some knowledge about their own shape, introducing what we could call proprioceptive materials. The approach for building such materials is presented.

2.1.1 Sensors

First step is to provide angular adequate information for surface computation. For that purpose, the following microsensors arre used.

- Microaccelerometers are able to provide the angle between the sensor and the vertical (as long as the sensor is quite static).
- Micromagnetometers are able to provide angular information with the earth magnetic field (when no magnetic pertubations around them occur).

These sensors have to be combined as a biaxial or a triaxial way, in order obtain the exact orientation of the measure point in the space (Fontaine et al., 2003). Five different measure from sensors are necessary to have the exact orientation (three accelerometers in a triaxial organization, and two magnetometers in a biaxial way). This study allows the creation of the prototype.

2.1.2 The Ribbon

Our new generation ribbon has been developed with the considerations above. The ribbon is equipped with a set of sixteen 3D microaccelerometers, alternating with a set of sixteen 2D micromagnetometers (AMR type sensors from Honeywell or similar). They are mounted on a flexible PCB ribbon. The distance between the sensors is nearly 25 mm. Such arrangement of the sensors allows gaining complete tangential information (not exactly at each sensor location, but for a set of two adjacent sensors). The sensors are read via a SPI serial bus, which allows a lot of sensors (see Figure 1). This ribbon is also easy to use thanks to its Bluetooth connection to the host computer. Finally, a software driver has been designed which allows to sequentially read all sensor values at different sampling

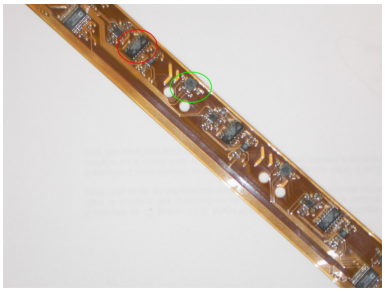

Figure 1: Ribbon of sensors able to provide 3D tangential data.

rates. In fact, the current ribbons are essentially prototypes that have been used for demonstration and validation purpose. Some technological issues are currently being addressed concerning sensor embedding in ribbons.

- Connections: we want to connect wires to a possibly great number of sensors. Solutions already exist at the die scale, but not at larger scales (up to meters). Dedicated connection technologies are currently being studied.
- Reliability: as the ribbon is planned to be flexible, most existing technologies do not apply. We are also studying various solutions to get such reliability.

Our final goal is to be able to produce ribbons and surfaces embedding possible large sensors areas, while keeping the advantage of low cost sensors.

2.1.3 The Ribbon Curve

The ribbon described above is able to provide its own shape. More precisely, methods have been developed to reconstruct curves via data from the ribbon, the curve being denoted *ribbon curve* (see Appendix A). Data are tangential data at sensors' positions, and distances between sensors along the ribbon. Let us notice that we do not have any information concerning absolute positions of any points of the ribbon, such that the ribbon curves reconstructed are unique up to their starting point.

2.2 Surface Acquisition Process

We have to acquire a surface via a ribbon of sensors, thus we have to reconstruct a surface from a finite number of ribbon curves laying on it. As it does not exist an intrinsic parameterization for surfaces (contrary to the curves with the arc-length parameter), we will keep the linear organization of sensors, and the ribbons are then a natural way to acquire surfaces. The question is thus as follows : how can we organize curves on a surface in order to know it ? Two

kinds of organization appear. The first one is a mesh of ribbons, where sensors are on the intersections. The surface is known by two families of curves in two complementary directions, so that we have a tensorial topology of the surface. This problem is well posed but this acquisition system is not really easy to use (how can we put it on non-developable surfaces? How can we put ribbons to cross exactly on sensors' positions?). So, in a more general case, we consider a second acquisition system, which consists in one family of ribbons in the same direction.

More precisely, we fix ribbons in the same direction on a mobile surface. Figure 2 shows an example of acquisition process with four parallel ribbons (in red), with sensors represented in black squares. In that case, ribbon curves are reconstructed independently, thus we have to fix their relative position with each other: we use an additional ribbon in the transversal direction, denoted *reference ribbon* linking all starting points A_k: thus we have a *comb structure* of ribbons to acquire a surface.

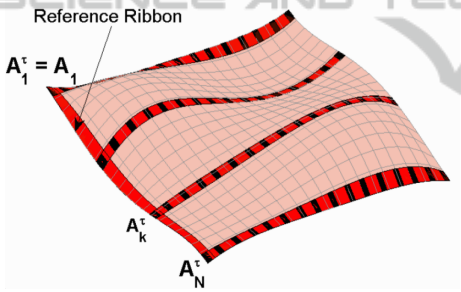

Figure 2: Surface acquisition process with 4 ribbons.

These ribbons give at each sensors' point tangential information (two vectors at sensors' position: $\mathbf{t}_k^\tau$ tangential vector of the ribbon curve, $\mathbf{b}_k^\tau$ binormal vector of the ribbon curve in the tangent plane (ribbon seen as a surface, equivalent to the surface to acquire at these points) (see Figure 3).

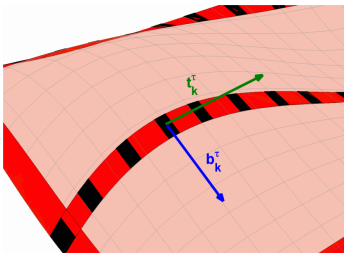

Figure 3: Tangential data given by sensors : unit tangent vector $\mathbf{t}_k^\tau$ and unit binormal vector $\mathbf{b}_k^\tau$.

When the surface is moving, ribbons are following the surface deformations. The surface is thus known via the moving curves laying on it. The figure 5-left illustrates the process.

The physical surface is then described with the flow of the tangential constraints (given by sensors on ribbons), with length constraints along the ribbons. The sensors are organized in a comb structure, with tangential data in both directions, but length constraints in only one direction (the ribbon curves direction).

3 SURFACE RECONSTRUCTION

As the surface acquisition process – with a comb structure – induces a tensorial structure on the physical surface, we consider the following reconstruction strategy.

At each time position :

1- we reconstruct the 3D ribbon curves from sensors data and length constraints,

2- these ribbon curves are adjusted according the comb structure,

3- from which we deduce the transversal 3D curves from sensors' data, but without any length information,

4- finally, the surface is filled by a standard cubic Coons process.

The main strategy is thus to follow the animated/deformed ribbons.

Step 1 has been validated in case of static reconstruction but could be time expensive. So, for real time reconstruction, the 3D ribbon curves at time position $\tau+\Delta\tau$ are deduced from the 3D ribbon curves at time position τ by an iterative/minimisation process. Precisely, Step 1 splits into two phases.

1a- *Initialization* – At time position $\tau = 0$, the 3D initial ribbon curves are reconstructed from the method described in Appendix A.

1b- *Iterative step* – The 3D ribbon curves at time position $\tau+\Delta\tau$ are deduced by an updating process from the tangential data of sensors at time $\tau+\Delta\tau$ and the sensors' position at time τ.

Notice that each ribbon curve is reconstructed up to an arbitrary starting point, in Steps 1a and 1b. These ribbon curves are then adjusted in Step 2 by using the reference ribbon curve. Finally, the whole reconstruction process will produce a C^1 surface.

3.1 Ribbon Curves Reconstruction

As Step-1a is detailed in Appendix A, we now focus on the iterative Step-1b. Assume we have $N+1$ rib-

bons (one of them being the reference ribbon curve), each of these ribbons being equipped with $n+1$ sensors numbered from 0 to n.

Considering any of these ribbons, each segment ribbon curve $\mathbf{r}_k^{\tau+\Delta\tau}(s)$ between sensor k and sensor $k+1$, at time position $\tau+\Delta\tau$, is modeled, as a cubic Hermite curve (see Appendix B)

$$\mathbf{r}_k^{\tau+\Delta\tau}(t) = \mathrm{H}[\mathbf{p}_k^{\tau+\Delta\tau}, \mathbf{p}_{k+1}^{\tau+\Delta\tau}, \mathbf{t}_k^{\tau+\Delta\tau}, \mathbf{t}_{k+1}^{\tau+\Delta\tau}; s_k, s_{k+1}](t)\,, \tag{1}$$

where :

- ◇ points $\mathbf{p}_k^{\tau+\Delta\tau}$, $\mathbf{p}_{k+1}^{\tau+\Delta\tau}$ are the *unknown* positions of sensors k and $k+1$ at time position $\tau+\Delta\tau$,
- ◇ vectors $\mathbf{t}_k^{\tau+\Delta\tau}$, $\mathbf{t}_{k+1}^{\tau+\Delta\tau}$ are the (updated) tangential information along the curve provided by sensors k and $k+1$ at time $\tau+\Delta\tau$,
- ◇ s_k, s_{k+1} are the arc length positions of sensors k and $k+1$ along the ribbon.

Then, the length constraints between sensors along the ribbon provide additional relations

$$\int_{s_k}^{s_{k+1}} \|\frac{\mathrm{d}}{\mathrm{d}t}\mathbf{r}_k^{\tau+\Delta\tau}(t)\|\,\mathrm{d}t = s_{k+1}-s_k\,, \tag{2}$$

for $k=0,\ldots,n-1$, at each time $\tau+\Delta\tau$. Expanding these integrals yield non linear constraints. Furthermore, as equations (2) do not have a unique solution, we consider the supplementary minimization constraints for $k=0,\ldots,n-1$

$$\min \int_{s_k}^{s_{k+1}} \|\frac{\mathrm{d}^2}{\mathrm{d}t^2}\mathbf{r}_k^{\tau+\Delta\tau}(t)\|^2\,\mathrm{d}t\,. \tag{3}$$

Finally, as constraints (2) and (3) allow to determine uniquely one of the two unknown position points of each segment ribbon curve, the method for the ribbon curve reconstruction proceeds iteratively as follows for each curve.

- Choose point $\mathbf{p}_0^\tau$ as starting point $\mathbf{p}_0^{\tau+\Delta\tau}$ of the ribbon curve.
- For each segment ribbon curve $\mathbf{r}_k^{\tau+\Delta\tau}(s)$, $k=0,\ldots,n-1$, compute the ending point $\mathbf{p}_{k+1}^{\tau+\Delta\tau}$ from relations (1) with the updated vectors $\mathbf{t}_k^{\tau+\Delta\tau}$, $\mathbf{t}_{k+1}^{\tau+\Delta\tau}$, and the (previously computed) starting point $\mathbf{p}_k^{\tau+\Delta\tau}$, from constraints (2) and (3). This minimization step is initialized with the previous point $\mathbf{p}_{k+1}^\tau$.

The Hermite definition (1) insures that the reconstructed ribbon curves will be C^1. Moreover, the *energy constraint* (3) on each segment ribbon curve insures to get a smooth ribbon curve among the family of curve solutions, i.e., C^1 cubic splines. Notice that these C^1 splines are not the classical ones as the initial data are tangent directions instead of 3D points.

3.2 Comb Structure Updating

As each ribbon curve is reconstructed up to an arbitrary starting point in the previous steps, we are now faced to adjust these curves according the reference ribbon curve.

This step is based on the two following points.

- The reference ribbon curve is reconstructed up to (the reference) point $A_1^\tau = A_1$ at each time position τ, see Figure 2. So that the whole surface will be reconstructed with respect to that point.
- Then, each "orthogonal" ribbon curve is translated in order its starting point match with the corresponding point A_k^τ.

3.3 Transversal Curves

At this point, we know at each time position the sensor's 3D position on each ribbon curve together with its associated transversal tangential information: the binormal vector, see Figure 3.

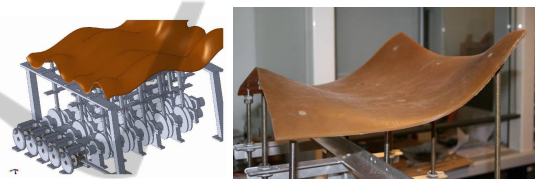

Figure 4: Future physical testing framework device.

Denoting more precisely by $\mathbf{p}_{k,j}^\tau$ the 3D position of sensor k on the ribbon curve j and by $\mathbf{b}_{k,j}^\tau$ the associated unit binormal vector, at each time position τ, we consider the cubic Hermite curve (see Appendix B) joining sensors k on ribbon curves j and $j+1$

$$\begin{aligned}&\mathbf{x}_{k,j}^\tau(t) \\ &=\mathrm{H}[\mathbf{p}_{k,j}^\tau, \mathbf{p}_{k,j+1}^\tau, \lambda_{k,j}^\tau \mathbf{b}_{k,j}^\tau, \lambda_{k,j+1}^\tau \mathbf{b}_{k,j+1}^\tau; t_j, t_{j+1}](t)\,,\end{aligned} \tag{4}$$

with $t_j = j-1$ and where $\lambda_{k,j}^\tau$ are positive coefficients associated with sensor k of the ribbon curve j at time position τ.

Then, considering the C^1 spline curve $\mathbf{x}_k^\tau(t)$, composed of segment curves $\mathbf{x}_{k,j}^\tau(t)$, the following minimization energy

$$\min \int_0^{N-1} \|\frac{\mathrm{d}^2}{\mathrm{d}t^2}\mathbf{x}_k^\tau(t)\|^2\,\mathrm{d}t\,, \tag{5}$$

leads to determine unique values for coefficients $\lambda_{k,j}^\tau$, producing smooth C^1 Hermite interpolating transversal curves.

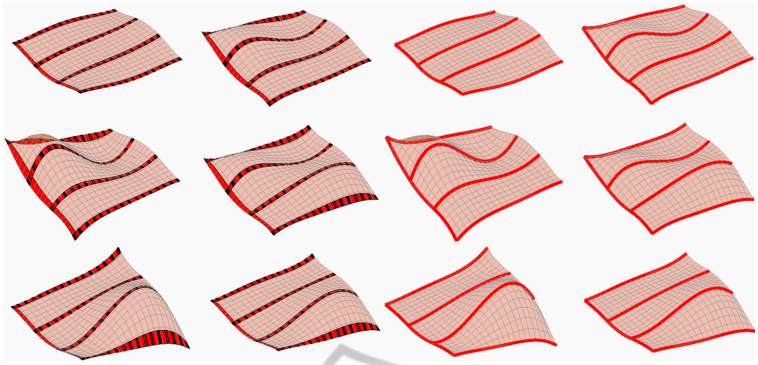

Figure 5: Left: animated analytical surface – Right: the reconstructed animated surface.

3.4 Surface Filling

At this point, the physical surface is reconstructed/modeled by a network of two families of "orthogonal" C^1 spline curves meeting at sensors' position, delimiting thus a set of $n(N-1)$ curvilinear rectangles.

Each of these curvilinear rectangles is then filled by a partially bi-cubically blended Coons process (Coons, 1974), producing a G^1 global surface.

Notice that this whole reconstruction process allows to faster refresh the display of the reconstructed surface, by only considering the previous network of "orthogonal" curves as a mesh approximating the surface.

4 CONTROL AND VALIDATION

The validation of such methods requires to compare the physical deformed surfaces and the reconstructed shapes at each time position, and clearly, a visual control is not sufficient. We describe here the experimental device under development for this purpose.

4.1 Experimental Device

We are currently developing a physical testing framework surface (see Figure 4), animated and controlled by a mechanical device. The surface motion is acquired by an optical system, providing an external reliable control.

By placing ribbons of sensors on this testing framework surface, according the process described in Section 2.2, we will acquire a network of animated spatial curves on this surface, allowing to compare the reconstructed surface by our process with the "optical surface" reconstructed from the external acquisition optical system.

Furthermore, the acquisition process of moving surfaces is intricate and requires a precise methodology. While the surface is moving, the physical ribbon will not keep an intrinsic position on the surface and will slip on the surface. Precisely, it is proved that these ribbons actually follow geodesic curves on the physical surface. Thus, when the surface is deformed, the ribbons slip in order to remain a geodesic on the surface. This is not a blocking point for our method as we need only distance information of the starting points of the curves, the ribbons remaining fixed at the origin.

4.2 Computed Examples

The animated analytical surface described in Figure 5-left is reconstructed using our process, see Figure 5-right.

An error is estimated between the animated analytical model of the surface and the reconstructed animated surface at some time position. Precisely, at each time position τ, the error is computed at sensors' position as

$$E(\tau) = \frac{100}{(n+1)NL_{rib}} \sum_{j=1}^{N} \sum_{k=0}^{n} \|\tilde{\mathbf{p}}_{k,j}^{\tau} - \mathbf{p}_{k,j}^{\tau}\|$$

where $\tilde{\mathbf{p}}_{k,j}^{\tau}$ and $\mathbf{p}_{k,j}^{\tau}$ are respectively the sensor's position on the physical surface and on the reconstructed surface, and where L_{rib} is the ribbon's length.

Figure 5 exhibits an example with a mean error equal to 1.68%, comprised in the interval $[1.18, 2.57]$, on a sample of 120 time positions.

5 CONCLUSIONS

A strategy for the acquisition of animated surfaces via a ribbon of sensors has been developed in this paper. The method is based on a comb structure of the reconstructed ribbon curves according a reference curve.

This approach allows to adjust the network of the reconstructed curves running on the surface and to get a "coherent" mesh interpolating the animated surface by an updating process from the previous time position. The method has been tested on an animated analytical surface.

Then, in order to validate the method in the general case of a physical animated surface, a testing framework surface is under development, so that, performance comparisons with real physical data have not been realized yet. Anyway, the first experiments have highlighted some practical difficulties concerning the implementation of the acquisition process. Essentially, we have to ensure a permanent smooth contact between the ribbon and the animated surface. Solutions (i.e., smoother and more flexible ribbons,...) are on progress.

REFERENCES

Coons, S. (1964). Surfaces for computer aided design. *Technical Report, M.I.T.,1964, Available as AD 663 504 from the National Technical Information service, Springfield, VA 22161*.

Coons, S. (1974). Surface patches and b-spline curves. *Computer Aided Geometric Design, In R. Barnhill and R. Riesenfeld editors, Academic Press*.

Farin, G. (2002). *Curves and Surfaces for CAGD - Fifth Edition*. Academic Press.

Fontaine, D., David, D., and Caritu, Y. (2003). Sourceless human body motion capture. In *Proc. Smart Objects Conference (SOC'03)*.

Hoschek, J. (1983). Dual bézier curves and surfaces. *Computer Aided Geometric Design, North Holland*, pages 147–156.

Hoshi, T. and Shinoda, H. (2008). 3d shape measuring sheet utilizing gravitational and geomagnetic fields. In *Proceeding of the SICE Annual Conference 2008*. The University Electro-Communications, Japan.

Nielson, G. (2004). ν-quaternion splines for the smooth interpolation of orientations. *IEEE Transactions on visualization and computer graphics*, 10(2):224–229.

Peters, J. (1990). Local smooth surface interpolation: A classification. *Computer Aided Geometric Design*, 7:191–195.

Sarraga, R. F. (1987). G1 interpolation of generally unrestricted cubic bézier curves. *Computer Aided Geometric Design*, 4:23–39.

Shirman, L. A. and Séquin, C. H. (1987). Local surface interpolation with bézier patches. *Computer Aided Geometric Design*, 4:279–295.

Sprynski, N., Lacolle, B., David, D., and Biard, L. (2007). Curve reconstruction via a ribbon of sensors. In *Proceeding of the 14th IEEE International Conference on Electronics Circuits and Systems*. ICECS, Marrakech, Maroc.

APPENDIX

A: Initial Reconstructed Curves. A 3D curve $C(s) = (x(s), y(s), z(s))$, parameterized with respect to its arc-length s satisfy $|C'(s)| \equiv 1$, so that the derivative curve $C'(s)$ is a curve lying on the unit sphere. Initial data are unit tangential vectors at points with assigned arc length parameters. The methodology is thus as follows.

- First, we interpolate data using cubic splines on the sphere, leading to the derivative curve $C'(s)$.
- Then, by integration we get a solution for $C(s)$.

Cubic splines on the unit sphere (see (Nielson, 2004)) are an extension of the usual B-splines in the euclidian space. The main differences are the following.
◇ The evaluation of the control polygon of cubic splines on the spherical space requires to solve a non linear system through an iterative algorithm.
◇ The usual De Casteljau algorithm, based on linear interpolations, has to be replaced by the *spherical interpolation*

$$Slerp(\mathbf{a},\mathbf{b},t) = \frac{\sin((1-t)\theta)\mathbf{a} + \sin(t\theta)\mathbf{b}}{\sin(\theta)},$$

where $\mathbf{a}$ and $\mathbf{b}$ are two unit vectors, θ the angle between vectors $\mathbf{a}$ and $\mathbf{b}$, and $t \in [0,1]$.

It is proved in (Sprynski et al., 2007) that this construction is invariant under rotations and scaling, and that these spherical splines minimize a combination of the curvature κ_1, the torsion κ_2, and the variations of the curvature, precisely

$$\min \int (\kappa_1'^2 + \kappa_1^2(\kappa_1'^2 + \kappa_2^2)),$$

which gives physical sense to the reconstruction.

B: Cubic Hermite Interpolation. Given spatial points $\mathbf{p}_0$ and $\mathbf{p}_1$ associated with tangent vectors $\mathbf{t}_0$ and $\mathbf{t}_1$, together with two parameters α_0 and α_1 ($\alpha_0 < \alpha_1$), there exists a unique cubic spatial parametric curve $\mathbf{r}(t)$ such that

$$\mathbf{r}(\alpha_0) = \mathbf{p}_0\,,\ \mathbf{r}(\alpha_1) = \mathbf{p}_1\,,\ \mathbf{r}'(\alpha_0) = \mathbf{t}_0\,,\ \mathbf{r}'(\alpha_1) = \mathbf{t}_1\,.$$

Precisely, $\mathbf{r}(t)$ is defined by

$$\begin{aligned}\mathbf{r}(t) &= H_0(\hat{t})\,\mathbf{p}_0 + H_1(\hat{t})\,\mathbf{p}_1 \\ &\quad + (\alpha_1-\alpha_0)H_2(\hat{t})\,\mathbf{t}_0 + (\alpha_1-\alpha_0)H_3(\hat{t})\,\mathbf{t}_1\,,\end{aligned}$$

with $\hat{t} = \frac{t-\alpha_0}{\alpha_1-\alpha_0}$ and where functions φ_j are the cubic Hermite polynomials (Farin, 2002) on the interval $[0,1]$, and $\mathbf{r}(t)$ and is denoted shortly by

$$\mathbf{r}(t) = \mathrm{H}[\mathbf{p}_0,\mathbf{p}_1,\mathbf{t}_0,\mathbf{t}_1;\alpha_0,\alpha_1](t)\,.$$